Research Square

Preprints are preliminary reports that have not undergone peer review.
They should not be considered conclusive, used to inform clinical practice,
or referenced by the media as validated information.

Insects as biosamplers of fine and ultrafine particles in urban environments

D. Meza-Figueroa

diana.meza@unison.mx

Universidad de Sonora

Francisco Berrellez-Reyes

Secretaría de Ciencia, Humanidades, Tecnología e Innovación, SECIHTI

Alejandro Valencia-Meza

Universidad de Sonora

Luis Fernando Valdez-Ojeda

Instituto de Ecología

B. González-Grijalva

Universidad de Sonora

Benedetto Schiavo

Universidad Nacional Autónoma de México

Paula Villarreal-Cantú

Procuraduría Ambiental del Gobierno del Estado de Sonora

Carmen Isela Ortega-Rosas

Universidad Estatal de Sonora

Research Article

Keywords: Wasp, honey bee, nanoparticle, air pollution, AFM, SEM-EDS

Posted Date: May 22nd, 2026

DOI: https://doi.org/10.21203/rs.3.rs-9545141/v1

License: This work is licensed under a Creative Commons Attribution 4.0 International License.
Read Full License

Additional Declarations: No competing interests reported.

Abstract

Although several insects can accumulate particles, most published research focuses on *Apis mellifera* (honey bee). In this study, we assess the efficiency of four insect species in capturing fine and ultrafine particles, namely the bee *Apis mellifera* (Apidae), the wasps *Cerceris* sp. (Crabronidae) and *Agenioideus* sp. (Pompilidae), and the fly *Sarcophaga* sp. (Sarcophagidae). All insects were captured alive at the same site near a high-traffic road in a city with a semi-arid climate in Mexico. We used a scanning electron microscope and an atomic force microscope to characterize the size and shape of particles adhering to insect wings and legs. Statistical analysis shows that *Agenioideus* and *Sarcophaga* capture elongated particles with higher aspect ratios, whereas *Apis mellifera* and *Cerceris* capture more rounded particles. The particle size distribution shows average wing sizes of 1.21 μm for *Apis mellifera*, 1.43 μm for *Agenioideus*, 1.79 μm for *Sarcophaga*, and 720 nm for *Cerceris*. Nanoparticles were predominantly found on the legs of *Cerceris*. Adhesion force on wings, measured by atomic force microscopy, was highest for *Cerceris* (60 nN) and lowest for *Sarcophaga* (11 nN). Identified particles mostly correspond to traffic sources, including particles enriched in Zr, Ce, Pb, Sb, Br, Fe, and Ba. This work highlights the potential of *Cerceris* as a biosampler for UFP in urbanized environments.

1.Introduction

Particulate matter (PM) air pollution was reported as the leading contributor to the global disease burden in 2021 (Brauer et al., 2024). The adverse health effects of PM smaller than 2.5 μm in diameter have been widely documented (World Health Organization, 2021), but recent studies raise concerns about human exposure to ultrafine particles (UFP) with diameters smaller than 0.1 μm (Bhardwaj et al., 2026). UFP can enter the bloodstream and reach crucial organs, including the brain (Schraufnagel, 2020), and some studies link UFP to systemic inflammation and oxidative stress (Leikauf et al., 2020). In recent years, interest has grown in using biological organisms as biosamplers for atmospheric fine (< 2.5 μm) and ultrafine (< 100 nm) particles. This trend reflects the growing recognition that these particles are difficult to characterize due to challenges in extraction methods (Berrellez-Reyes et al., 2025; Gallego-Hernández et al., 2020), yet they represent a hazardous component of air pollution. UFP occur by number rather than by mass, and their extremely high surface-to-mass ratio allows them to adsorb toxic metals, organic compounds, and persistent radicals (Kwon et al., 2020). Their small aerodynamic diameter facilitates long atmospheric residence and deep penetration into biological tissues, enabling them to cross epithelial barriers and enter the bloodstream (Kwon et al., 2020; Charpinel et al., 2024). These traits, coupled with limited regulation and a lack of standardized detection protocols, make UFPs a growing concern for environmental and public health (Flood-Garibay et al., 2023). Although toxicological studies often emphasize human exposure, laboratory evidence also demonstrates that air pollution can disrupt physiological processes in invertebrates (Charpinel et al., 2024). Such findings reinforce that UFPs act as biologically active agents across trophic levels, supporting the need for natural organisms that can integrate and reflect ambient particle exposure. Insects, in particular, provide an effective biological interface for this purpose. Their abundance, ubiquity, and close interaction with air, vegetation, and soil make them powerful bioindicators of environmental pollution (Chowdhury et al., 2023; Papa et

al., 2025). Because insects occupy a broad range of ecological niches and trophic roles, they collectively experience—and record—pollutant exposure in ways that stationary sampling devices cannot. Their morphology and surface chemistry allow particulate adhesion, while their flight and foraging behaviors determine exposure routes, providing fine- scale, spatially integrated information on air quality. In other words, they function as biological collectors that sample pollution within the microenvironments they inhabit.

Among insects, flying taxa are particularly well suited to capture airborne UFPs because of a fundamental biophysical mechanism: triboelectric charging during flight. As insect wings beat through air, friction between the cuticle and air molecules generates a positive electric charge; many airborne particles and plant surfaces carry negative charges. The resulting Coulombic attraction promotes efficient adhesion of small particles—including pollens and metallic aerosols—to the insect's body (Meacci et al., 2025). This phenomenon, well documented in *Apis mellifera*, likely extends to other pilose flying insects, such as wasps (Skaldina et al., 2023), although bees remain the most studied model (Meacci et al., 2025; Moniuszko et al., 2025). Their dense pilosity, waxy cuticle, and predictable foraging behavior make them exceptionally efficient mobile samplers. Consequently, bees integrate particulate exposure across the spatial extent of their flight paths, capturing both temporal and microscale variability that stationary collectors often miss.

Apis mellifera has been widely used as a bioindicator of environmental pollutants, including metals, pesticides, and particulate matter (Negri et al., 2015; Papa et al., 2021). Using scanning electron microscopy (SEM) and energy-dispersive X-ray spectroscopy (EDS), researchers have shown that particles adhering to bee wings and legs match the chemical signatures of local anthropogenic and geogenic sources (Negri et al., 2015; Papa et al., 2025). More recent analyses reveal that bee-captured particulates mirror the geochemical fingerprints of surrounding dust, with nanoscale fractions (60–480 nm) enriched in vanadium, chromium, and lead in Mexico City and in cerium and zirconium in Hermosillo (Meza-Figueroa et al., 2024). These studies confirm that honey bees serve as active biosamplers of fine and ultrafine particles and that microscopy-based approaches can quantitatively link particle morphology and chemistry to urban emission sources.

However, restricting biomonitoring to *Apis mellifera* (honey bees) may overlook the ecological and behavioral diversity that shapes particle exposure in other insects. Honey bees primarily interact with floral aerosols and rarely contact soil, decaying matter, or prey surfaces, sampling only a narrow subset of the airborne particle environment (Meacci et al., 2025). Exploring other taxa as UFP biosamplers could reveal complementary exposure pathways and capture distinct particulate fractions. Insects' evolutionary diversification offers unique comparative advantages for such studies. Variations in cuticle microstructure, hair density, wing morphology, feeding strategy, and habitat preference all influence the types and quantities of particles that adhere to the body (Chowdhury et al., 2023; Meacci et al., 2025). Even minor differences in daily activity patterns or vertical flight height can alter exposure to specific particle sizes or sources, effectively making each species a distinct biomonitoring model.

Therefore, biomonitoring frameworks seeking to characterize UFP distribution and composition should use a complementary set of species representing contrasting ecological functions. A multispecies approach increases novelty and ecological resolution by capturing exposure across multiple behavioral strata and microhabitats. Pollinators interact with floral aerosols at the canopy level; parasitoids and predators contact soil and prey surfaces near the ground; and saprophagous species engage with decomposing substrates rich in resuspended particulates. Comparing these ecological guilds can highlight how microenvironmental context shapes UFP accumulation and retention, aligning with broader "One Health" perspectives that integrate human, animal, and ecosystem well-being.

Insects are among the most ecologically diverse groups in terrestrial ecosystems, including urban environments, making them ideal for constructing a comparative framework. Their diversity allows the deliberate selection of species with distinct ecological roles—saprophagous, pollinators, predators, detritivores, mycophagous, or parasitoids (Chowdhury et al., 2023; Marshall, 2018). Following this rationale, we selected common urban representatives from different functional groups to test whether ecological specialization influences the type and quantity of UFPs captured. Specifically, the bee *Apis mellifera* (Apidae, hereafter *Apis*) was included as a pollinator focused on nectar and pollen collection (Yadav et al., 2017); the wasps *Cerceris sp.* (Crabronidae) and *Agenioideus sp.* (Pompilidae) as parasitoids of beetles and spiders, respectively (Nelapa et al., 2013; Shimizu, 1997); and the fly *Sarcophaga sp.* (Sarcophagidae) as a saprophagous species whose larvae develop in decomposing organic matter (Perez-Moreno et al., 2006). Together, these taxa represent a functionally diverse assemblage of biological collectors exposed to distinct particle reservoirs within urban habitats. Using SEM imaging, statistical analyses of particle morphometry and size distribution, and atomic force microscopy (AFM) to explore surface adhesion, we evaluated how ecological traits mediate UFP accumulation and assessed the feasibility of a multi-species insect biomonitoring framework for characterizing airborne fine and UFP pollution.

2. Materials and Methods

2.1 Study site, sampling, and specimen collection

Insects were collected in a pollinator garden at the intersection of two high-traffic avenues, including a vehicular bridge, on the University of Sonora campus (Figure S1). This site was selected because it is directly influenced by traffic-related air pollution, and on-road vehicles are the principal source of UFP emissions in urban environments (Chauhan et al., 2024). Sampling was conducted in spring 2025 (March-April), coinciding with the emergence of adult bees and wasps in the region and with increased atmospheric particulate matter levels. Collections were performed during weekday daytime hours, when vehicular emissions typically peak.

To minimize contamination and prevent loss of surface-adhered UFPs, insects were captured directly in flight using a Malaise trap (Fig. 1), avoiding contact with vegetation or artificial substrates. In a standard Malaise trap, flying insects are intercepted by a horizontal mesh and typically move upward toward the

white ceiling due to positive phototropism, where they are collected in a container with 70% ethyl alcohol. For this study, the trap design was modified by omitting the alcohol-filled container to prevent dissolution or removal of adhered particles. Instead, insects were continuously monitored and manually captured in flight using an entomological net.

Immediately after capture, each specimen was placed in a sterile polypropylene vial and transported to the laboratory. Specimens were euthanized by freezing and then mounted on entomological pins for taxonomic identification and microscopic analyses. This handling protocol was designed to minimize artefactual gain or loss of particles from body and wing surfaces before SEM and AFM analysis.

Taxonomic identification was conducted using standardized morphological keys. Specimens were initially assigned to order based on the criteria of Triplehorn & Johnson (2004). Of the four individuals analyzed, two were identified as Diptera and two as Hymenoptera. Wings from these specimens were selected for detailed particle-size and morphometric analysis. Each specimen therefore represents an individual collector of atmospheric particles, from which numerous adhered particles were measured.

Dipteran specimens were assigned to the family Sarcophagidae using McAlpine (1981) and subsequently identified to the genus *Sarcophaga* following Shewell (1987). Among Hymenoptera, family-level identification was assigned to Pompilidae and identified as *Agenioideus* (Wasbauer & Kimsey, 1985); another to Crabronidae and identified as *Cerceris* (Kim, 2015); and two specimens to *Apis* (Apidae).

These taxa form a functionally diverse assemblage comprising a pollinator (*Apis*), parasitoid wasps (*Agenioideus, Cerceris*), and a saprophagous fly (*Sarcophaga*), enabling comparison of particle capture across contrasting ecological niches. Figure 1 shows the Malaise trap design, the sampling site, and four representative specimens for detailed analysis: (A) Crabonidae-*Cerceris*, (B) Sarcophagidae-*Sarcophaga*, (C) Pompilidae-*Agenioideus*, and (D) Apidae-*Apis*.

2.2 Particle characterization by SEM-EDS and AFM

Wings were carefully removed with a sterile micro-scalpel and handled exclusively with antistatic tweezers to avoid dislodging adhering particles. Each wing was sectioned into smaller fragments—restricted to interveinal zones to favor flat regions suitable for scanning—and mounted on aluminum SEM stubs using transparent double-sided adhesive tabs that were previously cleaned with compressed nitrogen gas. No conductive coating was applied to preserve the morphology and chemical composition of surface-adhered particles for SEM–EDS analysis. SEM imaging was performed on a Phenom ProX Thermo Scientific at an electron acceleration voltage of 15 kV, operating in backscattered electron (BSE) mode. Metallic particles were identified based on Z-contrast, in which low atomic number substrates (chitin) appear dark and high atomic number particles appear bright gray to white. Particle size was expressed as the circle equivalent diameter (CED), and morphology parameters, including aspect ratio (AR) and circularity, were obtained using the ParticleMeter software on the Phenom ProX.

For AFM scanning, mounted wing pieces were allowed to equilibrate at room temperature in a desiccator for 24 h to minimize humidity-related drift. All samples were stored in closed containers between imaging sessions to prevent additional particulate deposition. Wing topography was characterized using a Park Systems XE-Bio AFM coupled to a Nikon Ti-E inverted optical microscope, enabling precise localization of the scanning regions. Scans were acquired in contact mode using a PPP-CONTR probe (Nanosensors) with a nominal spring constant of 0.2 N m^{-1}, a tip radius < 10 nm, and cantilever dimensions of 450 µm × 50 µm × 2 µm.

Images were collected over 3–5 µm² areas at 0.5 Hz, with parameters chosen to resolve nanoscale cuticular elements while minimizing tip-induced deformation. Force–distance (F/D) curves were obtained from selected regions, recorded at 0.3 µm s^{-1} with 512-point resolution and a setpoint of 8.25 nN to evaluate adhesion forces. AFM thus provided quantitative nanoscale descriptors of surface roughness and local mechanical behavior that are directly relevant to particle–surface interaction potentials.

Because insect wings exhibit complex three-dimensional heterogeneity, a systematic approach was used to identify suitable scanning sites. Initial overview scans were conducted at 50, 20, and 10 µm², followed by high-resolution scans at 5 and 3 µm². Interveinal regions and areas between microtrichial clusters were prioritized to minimize topographical artifacts. Wing architectures included conical pillars averaging ~ 7 µm in diameter and ~ 20 µm in height, spaced ~ 65 µm apart (Ewunkem et al., 2023). These structures can exceed the scanner's Z-range and were therefore avoided.

For each specimen, surface roughness parameters Rq (root-mean-square roughness) and Ra (arithmetic mean roughness) were extracted using the manufacturer’s analysis software. Rq is sensitive to larger height deviations and pronounced nano- to microrelief, whereas Ra represents the mean absolute deviation from the reference plane. Together, these parameters characterize the effective contact landscape encountered by incoming particles during impact or sliding across the wing surface.

2.3 Statistics

All statistical analyses were performed in R (v.4.4; R Core Team), following a workflow designed to evaluate whether particle assemblages differed by insect genus in both their multivariate structure and their univariate traits. Individual particles were treated as observations describing the morphospace of particles transported by each insect specimen. Because particle morphometrics are intercorrelated quantitative descriptors, analyses were conducted on standardized (z-scaled) variables to allow direct comparison across traits and to avoid scale-driven distortions in multivariate space.

A principal component analysis (PCA) was performed using a correlation-matrix approach, appropriate when variables are measured on different scales (e.g., microns vs dimensionless shape descriptors). PCA was selected because it reduces the dimensionality of the morphometric dataset while preserving most of its variance, enabling visualization of particle-level patterns associated with each insect genus. This method assumes linear combinations of variables and is therefore well suited to continuous,

standardized morphometric data such as CED, AR, and circularity. The resulting ordination summarizes how particle shapes and sizes covary across insects, and PCA loadings were used to identify which traits drive differences among particle assemblages associated with the sampled insects.

To assess whether particle assemblages differed among insect genera, a permutational multivariate analysis of variance (PERMANOVA) was conducted using Euclidean distances on standardized variables. PERMANOVA is well suited to ecological and morphometric datasets because it does not assume multivariate normality—a property rarely met in biological particle measurements—and instead uses permutations to estimate significance. This method tests whether the centroid positions of particle assemblages associated with each genus in multivariate space differ beyond what would be expected by chance, thereby quantifying whether particle assemblages associated with different insects occupy distinct regions of morphometric space.

Because PERMANOVA can be sensitive to differences in within-group dispersion, we also assessed the homogeneity of multivariate dispersions using the betadisper test. This test evaluates whether the spread of samples around each group centroid varies across genera, ensuring that statistically significant PERMANOVA results reflect compositional differences rather than unequal within-group variances. Distances-to-centroid were retained to determine whether differences among particle assemblages arise from shifts in average particle profiles or from variation in particle heterogeneity.

To complement multivariate analyses, each morphometric descriptor was also examined individually using univariate statistical tests. Before hypothesis testing, normality and homogeneity of variance were assessed with the Shapiro–Wilk and Levene tests, respectively. When assumptions were met, differences across genera were tested with one-way ANOVA, followed by Tukey's HSD post hoc contrasts; when assumptions were violated, the nonparametric Kruskal–Wallis test and Dunn pairwise comparisons (Benjamini–Hochberg adjusted) were used. This dual approach ensures methodological rigor by adapting the statistical framework to the empirical distribution of each trait rather than imposing parametric assumptions. Means, standard errors, and confidence intervals were calculated to summarize central tendency and dispersion for each genus.

The combined multivariate–univariate statistical framework is well suited to particle adhesion datasets. PCA and PERMANOVA jointly assess whether particle assemblages associated with each insect differ in overall particle morphology, while univariate tests identify which specific traits (e.g., circularity or AR) drive those differences. This design captures both holistic and trait-specific patterns, strengthening ecological interpretations and providing a robust foundation for linking wing microstructure, behavior, and UFP capture. Because particles are nested within individual insects, statistical comparisons are interpreted as differences among particle assemblages associated with each sampled insect rather than as population-level differences among species.

3.Results and Discussion

3.1. Morphology and size of captured particles

The dataset is suitable for PCA, as the KMO sampling adequacy measure is 0.6, and the analysis meets Bartlett's sphericity test (at least one correlation between variables is significantly different from 0, two-tailed p-value < 0.0001). The PCA shows that the first two components account for 81.9% of the cumulative variance (Fig. 2). Component 1 contains 58% of the variance and explains morphological aspects of AR and circularity. Component 2 contains 23.9% of the total variance and explains particle size (CED). The ellipses for each genus overlap substantially, indicating that although there are distinct average trends, the internal variability within each genus is wide and the “morphological patterns” are not exclusive. Visually, *Agenioideus* appears to have the most extended ellipse (greater dispersion), *Sarcophaga*'s ellipse is also quite wide, while the ellipses for *Cerceris* appear more compact and for *Apis* they are intermediate. This fits with the idea that the genus explains part, but not all, of the morphological variation of the particles: there is considerable intragroup heterogeneity. Particle morphology is relevant to understanding the sources; irregular/angular particles with lower aspect ratio and circularity are commonly linked to natural or anthropogenic abrading processes such as milling or construction dust. On the other hand, soot particles forming chain-like aggregates of small particles, and spherical particles with AR and circularity close to 1, are related to combustion processes, such as oil combustion or vehicular exhaust emissions. Determining particle morphology is important for understanding their residence time in the atmosphere, since particles with high AR have a lower sedimentation rate than spherical or circular particles, remaining in suspension for longer periods. Furthermore, particle shape influences their ability to penetrate the respiratory system (Fatima et al., 2023).

The AR (Fig. 3) results indicate that particle assemblages associated with *Agenioideus* and *Sarcophaga* are characterized by more elongated or narrow particles (low AR values), whereas particles associated with *Apis* and *Cerceris* show higher median values, reflecting wider or near-rounded shapes (high AR values). Most paired comparisons are significant (indicated by bars marked ***, **** in Fig. 3). Ecologically, this suggests that the microstructure and/or the behavior of the sampled *Apis* and *Cerceris* individuals when in contact with plant surfaces may favor the retention of proportionally “rounded” particles, whereas particle assemblages observed on *Agenioideus* and *Sarcophaga* are associated with more elongated particles. In addition, circularity reveals differences among the insects studied. Particles observed on *Sarcophaga* wings show a higher abundance of low-circularity shapes, corresponding to more angular or irregular particles. Particles adhered to *Apis* and *Agenioideus* appear more circular, in agreement with the AR results. In summary, the particle assemblage associated with *Agenioideus* displays the highest proportion of elongated particles, while particles observed on *Sarcophaga* tend to be less elongated, and those associated with *Apis* and *Cerceris* include mixtures of both particle types.

Particle size results relate to CED. Statistical analysis of CED indicates that *Sarcophaga* retains the largest particles in wings, followed by *Apis*, whereas *Cerceris* tends to capture the smallest particles. CED values show average wing particle sizes of 1.21 µm for *Apis*, 1.43 µm for *Agenioideus*, 1.79 µm for *Sarcophaga*, and 720 nm for *Cerceris*.

Insects clean themselves using body parts such as legs to remove dirt from their antennae and appendages and to enhance olfactory acuity (Böröczky et al., 2013). In particular, wasps and bees have modified leg spines (strigils) for self-cleaning. Honey bees' hind legs are used to groom pollen from their bodies (Santos & Hartfelder, 2015). To further explore the capture of UFPs, we analyzed the legs and combs of *Apis* and *Cerceris*, because, according to the statistical results, these species capture the smallest particles (Fig. 4).

Apis' legs show a particle size range of 242 nm to 6.03 μm (Figure S2B), with a mean size of 1.92 μm (Table S1). The particle size distribution in *Cerceris'* legs ranges from 140 nm to 1 μm, with a mean size of 471 nm (Figure S3B, Table S2), highlighting Cerceris' efficiency *in* capturing submicron particles. Figure 5C shows that most submicron particles are spherical (circularity > 0.5), likely originating from combustion processes.

3.2. Adhesion force by AFM

AFM studies have demonstrated that pollen and silica spheres adhere more effectively to the wing surfaces of hydrophilic insects, such as the wasp *Scolia soror* and the butterfly *Eurema hecabe*, than to those of hydrophobic insects, such as the cicada *Thopha sessiliba* (Watson et al., 2012). Published research on the insect cuticle reveals properties that may explain its ability to capture pollutants, including superhydrophobicity, low adhesion, and self-cleaning (Böröczky et al., 2013; Vincent & Wegst, 2004; Wagner et al., 1996). Figure 6 shows the differences in adhesion among the four insects in this study. The order of adhesion strength on the cuticle was *Cerceris* (60 nN) > *Apis* (33 nN) > *Agenioideus* (15 nN) > *Sarcophaga* (11 nN). This finding aligns with the statistical interpretation and explains *Cerceris*'s efficiency in capturing UFP. Compared with previous studies, *Cerceris* exhibits similar adhesion strength on pollen (60 nN) and silica (50 nN) for the *Scolia* sp. Wasp (Watson et al., 2012).

The high efficiency of *Cerceris* in UFP retention stems from the synergistic interplay among surface topography, waxy cuticle properties, and local contact mechanics. As shown by 2D AFM topographic analysis (Fig. 7A), the low surface roughness of *Cerceris* (Rq = 7.04 nm; Ra = 5.56 nm) maximizes the real contact area at the particle-surface interface. According to nanopatterned surface adhesion models proposed by Burton et al. (2005), this increased contact area yields a significantly higher pull-off force (60 nN), thereby enhancing adhesion of nanometric particles. A similar trend is observed in *Apis* (Fig. 7B), which exhibits comparable roughness values (Rq = 9.18 nm; Ra = 6.99 nm) and an intermediate adhesion force of 33 nN.

In contrast, AFM topographic images of *Sarcophaga* (Fig. 7C) reveal a granular surface texture (Rq = 16.62 nm; Ra = 12.93 nm). Although these granular features may facilitate mechanical entrapment of larger micro-sized particles within cuticular interstitial spaces, they simultaneously reduce adhesion efficiency for UFP, as reflected in the lower measured adhesion force (11 nN). Consistent with adhesion-structure mechanisms described by Scholz et al. (2008), these granules act as mechanical spacers that increase the stand-off distance between nanoparticles and the cuticular surface, thereby weakening van

der Waals interactions. Furthermore, following the principle of size-dependent attachment, the substantially higher roughness and pronounced longitudinal ridges observed in *Agenioideus* (Fig. 7D; Rq = 41.91 nm; Ra = 33.43 nm) generate a roughness-induced detachment effect for ultrafine particles, with an adhesion force of 15 nN. Consequently, the biophysical surface profile of *Cerceris* promotes enhanced retention of traffic-related ultrafine particles, supporting its role as an effective bio-sampling taxon for urban air quality monitoring.

3.3.Particle composition

The SEM-EDS study identified particles associated with non-exhaust emissions from vehicular traffic in all insects studied. Figure 8 shows examples per species. Figures 8A and 8B highlight the *Cerceris* (wasp) efficiency in capturing fine particles associated with air pollution. Figure 8A shows a particle derived from the auto catalyst cover that also appears to include cordierite, an aluminosilicate that forms the ceramic monolith on which the Zr-Ce refractory coating is established. Particles containing Zr-Ce have been associated with emissions from the refractory coating of three-way catalysts (Meza-Figueroa et al., 2024; Navarro-Espinoza et al., 2021). Previously, the viability of wasps (German wasp *Vespula germanica* (F.) and common wasp *Vespula vulgaris*) as mobile samplers of particulate matter has been documented (Skaldina et al., 2023).

Particulate matter adhering to insect wings reflects atmospheric pollutants associated with urban sources. Figures 8B and 8C show the presence of breathable coarse and fine Pb-enriched particles attached to *Cerceris* and *Sarcophaga*, respectively. Coal combustion, non-exhaust traffic, industrial sources, and leaded paint are currently considered the main Pb sources in cities following the phasing out of leaded gasoline (Ye et al., 2022; Harvey et al., 2017). Exposure to lead, even at low levels, is considered a risk to human health because it is a neurotoxicant that can cause various disabilities (Ranjbar et al., 2023). *Agenoioideus* shows attached particles possibly related to brake pads (Ba-S, Fig. 8E) and an Fe-enriched particle (Fig. 8F).

Figures 8G and 8H show the variety of particles attached to *Apis*. Some particles appear to be calc-silicates of natural origin, mixed with Fe-oxides and rounded Si-particles from high-temperature combustion sources. In summary, all insects captured particles related to traffic sources. The main differences are in the amount of UFP particles, in descending order, starting with *Cerceris > Apis > Agenoioideus > Sarcophaga*.

4.Limitations of study

Due to the difficulty of capturing insects in flight, sampling was conducted at a single station. All specimens were collected at the same site and during the same sampling period, ensuring comparable environmental conditions and exposure to a shared atmospheric particulate matter matrix. Under this framework, the particles captured by each insect can be interpreted as parallel samples of the same urban polluted air. This allows a direct comparison of the types, sizes, and morphologies of particles retained by different taxa under equivalent exposure conditions. Differences among insects therefore

reflect how each biological surface interacts with and retains particles from the same environmental input, rather than differences in particle availability. Although the number of individuals analyzed is limited, the objective of this study is not to assess population-level variation but to characterize particle assemblages associated with each specimen and to evaluate how different insect taxa sample and retain particles. Future studies incorporating larger sample sizes, multiple sites, and seasonal variation will be necessary to evaluate the generality of these patterns.

5.Conclusions

All the insects evaluated allow for the characterization of UFPs adhering to their wings and legs using SEM and AFM without solvent extraction. This approach preserves particle morphology and composition and enables direct observation of particle assemblages associated with each specimen. Because all insects were collected at the same site and during the same sampling period, the particles observed can be interpreted as originating from a shared atmospheric environment. Under these conditions, the differences observed among insects do not reflect changes in particle availability but rather how each insect retains particles from the same media.

Although particle distributions overlap, consistent differences in size, shape, and composition are observed among taxa, suggesting that each insect captures different fractions of the available PM. AFM measurements show that adhesion strength varies among insects and aligns with differences in particle retention. Adhesive force is highest in *Cerceris*, which also shows the greatest capacity to capture UFPs. In contrast, lower adhesion values correspond to reduced particle retention in other taxa. Smaller particles are more frequently retained on legs than on wings, indicating that body structures may influence particle accumulation. In addition, *Cerceris* captures both metallic and non-metallic particles (including Si-rich spheres), whereas *Apis* shows a stronger association with metallic particles. Overall, these results support the use of insects as biological samplers of urban PM and show that using more than one species provides a more complete view of UFPs in urban atmospheric environments.

Declarations

Funding

This work was supported by the Secretariat for Humanities, Science, Technology and Innovation in Mexico (SECIHTI) Grant PRONACES 317557 to Diana Meza-Figueroa. The results of this paper are part of a postdoctoral fellowship provided by SECIHTI to Francisco Berrellez (supervised by Prof. Meza-Figueroa).

CrediT authorship contribution statement

D. Meza-Figueroa: Writing-original draft, Supervision, Resources, Methodology, Funding acquisition, Conceptualization. **F. Berrellez-Reyes**: Methodology, Formal analysis, Investigation. **A. Valencia-Meza**: Writing-original draft, Formal analysis, Conceptualization, Data curation. **L.F. Valdez-Ojeda**: Writing-

original draft, Investigation, Methodology, Formal analysis. **B. González-Grijalva**: Formal analysis, Methodology, Investigation. **B. Schiavo**: Writing-review & editing, Formal analysis, Conceptualization. **P. Villarreal-Cantú**: Methodology, Investigation. **C.I. Ortega-Rosas**: Writing-review & editing, Resources, Conceptualization, Investigation.

Acknowledgments

The authors gratefully acknowledge Dr. Erika Silva's support with the AFM.

References

1. Berrellez-Reyes, F., Schiavo, B., Gonzalez-Grijalva, B., Angulo-Molina, A., Meza-Figueroa, D. (2025). Characterization of soot and crystalline atmospheric ultrafine particles. Environmental Pollution 364, 125314. https://doi.org/10.1016/j.envpol.2024.125314
2. Bhardwaj, S., Bharti, A., Sharma, R.S., Mishra, S.K., Kumar, P., Ethayathulla, A.S., Singh, A., Mishra, V. (2026). Linking particulate matter exposure and neurological disorders: Evidence from epidemiology, biomarkers and mechanistic studies. Neurotoxicology 113, 103375. https://doi.org/10.1016/j.neuro.2025.103375
3. Böröczky, K., Wada-Katsumata, A., Batchelor, D., Zhukovskaya, M., Schal, C. (2013). Insects groom their antennae to enhance olfactory acuity. PNAS 110(9), 3615–3620. pnas.org/cgi/doi/10.1073/pnas.1212466110
4. Brauer, M., Roth, G.A., Aravkin A.Y., Zheng, P., Abate, K.H., Abate, Y.H., et al. (2024). Global burden and strenght of evidence for 88 risk factors in 204 countries and 811 subnational locations, 1990–2021: a systematic analysis for the global burden of disease study 2021. Lancet 403 (10440), 2162–2203.
5. Burton, Z., & Bhushan, B. (2005). Hydrophobicity, Adhesion, and Friction Properties of Nanopatterned Polymers and Scale Dependence for Micro- and Nanoelectromechanical Systems. Nano Letters, 5(8), 1607–1613. https://doi.org/10.1021/nl050861b
6. Charpinel A.M.M., Féres J.C., Barreto F.C.C. (2024). Effects of fine particulate matter air pollution on survival of Heliconiu ethilla (Godart, 1819). Scientific Reports 14(1), 29710. https://doi.org/10.1038/s41598-024-78347-w
7. Chauhan B.V.S., Corada K., Young C., Smallbone K.L., Wyche K.P. (2024). Review on Sampling Methods and Health Impacts of Fine ($PM_{2.5}$, ≤ 2.5 μm) and Ultrafine (UFP, PM0.1, ≤ 0.1 μm) Particles. Atmosphere 15, 572. https://doi.org/10.3390/atmos15050572
8. Chowdhury S., Dubey V.K., Choudhury S., Das A., Jeengar D., Sujatha B., Kumar A., Kumar N., Semwal A., Kumar V. (2023). Insects as bioindicator: A hidden gem for environmental monitoring. Frontiers in Environmental Sciences 11. https://doi.org/10.3389/fenvs.2023.1146052
9. Ewunkem, A.J., Beard, A.F., Justice, B.L., Peoples, S.L., Meixner, J.A., Kemper, W., Iloghalu, U.B. (2023). Honeybee wings hold antibiofouling and antimicrobial clues for improved applications in health care and industries. Microbiology 9(2), 332–345. https://doi.org/10.3934/microbiol.2023018

10. Fatima S., Mishra SK., Kumar U., Ahlawat A., Dabodiya TS., Khosla D. (2023). Role of morphology and chemical composition of PM for particle deposition in human respiratory system: A case study over megacity-Delhi. Urban Climate 47, 101344. https://doi.org/10.1016/j.uclim.2022.101344
11. Flood-Garibay, J., Angulo-Molina, A., Méndez-Rojas, M. (2023). Particulate matter and ultrafine particles in urban air pollution and their effect on the nervous system. Environmental Science: Processes & Impacts 4, https://doi.org/10.1039/d2em00276k
12. Gallego-Hernández, A.L., Meza-Figueroa, D., Tanori, J., Acosta-Elias, M., González-Grijalva, B., Maldonado-Escalante, J.F., Rochín-Wong, S., Soto-Puebla, D., Navarro-Espinoza, S., Ochoa-Contreras, R., Pedroza-Montero, M. (2020). Identification of inhalable rutile and polycyclic aromatic hydrocarbons (PAHs) nanoparticles in the atmospheric dust. Environmental Pollution 260, 114006. https://doi.org/10.1016/j.envpol.2020.114006
13. Harvey, P.J., Rouillon, M., Dong, C., Ettler, V., Handley, H.K., Taylor, M.P., Tyson, E., Tennant, P., Telfer, V., Trinh, R. (2017). Geochemical sources, forms and phases of soil contamination in an industrial city. Science of the Total Environment 505–514, 584–585. https://doi.org/10.1016/j.scitotenv.2017.01.053
14. Kim J.K. (2015). New records of two Nyssonini (Bembicinae: Crabronidae) specie from Korea, with a key to higher taxa of Sphecidae s. lat. occurring in Korea. Journal of Asia-Pacific Biodiversity 8, 222–226. https://doi.org/10.1016/j.apb.2015.09.001
15. Kwon H.S. (2020). Ultrafine particles: unique physicochemical properties relevant to health and disease. Experimental and Molecular Medicine 52, 1–11. https://doi.org/10.1038/s12276-020-0405-1
16. Leikauf, G.D., Kim, S.H., Jang, A.S. (2020). Mechanisms of ultrafine particle-induced respiratory health effects. Experimental & Molecular Medicine 52(3), 329–337. https://doi.org/10.1038/s12276-020-0394-0
17. Marshall, S.A. (2018). Beetles: The Natural History and Diversity of Coleoptera. Firefly Books (US) Incorporated, United States of America.
18. McAlpine J.F. (1981). Key to families-Adults. Manual of Nearctic Diptera, Vol. 1, 89–124. Research Branch, Agriculture and Agri-Food Canada, Canada.
19. Meacci, S., Corsi, L., Santecchia, E., Ruschioni, S. (2025). Harnessing Electrostatic Forces: A Review of Bees as Bioindicators for Particulate Matter Detection. Insects 16(4), 373. https://doi.org/10.3390/insects16040373
20. Meza-Figueroa, D., Berrellez-Reyes, F., Schiavo, B., Morton-Bermea, O., Gonzalez-Grijalva, B., Inguaggiato, C., & Silva-Campa, E. (2024). Tracking fine particles in urban and rural environments using honey bees as biosamplers in Mexico. Chemosphere, 363, 142881. https://doi.org/10.1016/j.chemosphere.2024.142881
21. Moniuszko, H., Przybysz, A., Boranski, M., Splitt, A., Jachula, J., Popek, R. (2025). Buff-tailed bumblebee, and underrated indicator of air pollution: a comparison of particulate matter

accumulation by *Bombus terrestris* L. and *Apis mellifera* L. Environmental Toxicology and Chemistry, 44(1), 282–293. https://doi.org/10.1093/etojnl/vgae020

22. Navarro-Espinoza, S., Meza-Figueroa, D., Guzmán, R., Duarte-Moller, A., Esparza-Ponce, H., Paz-Moreno, F., González-Grijalva, B., Álvarez-Bajo, O., Schiavo, B., Soto-Puebla, D., Pedroza-Montero, M. (2021). Release of Nanoparticles in the Environment and Catalytic Converters Ageing. Nanomaterials 11, 3406. https://doi.org/10.3390/nano11123406
23. Negri, I., Mavris, C., Di Prisco, G., Caprio, E., & Pellecchia, M. (2015). Honey bees (Apis mellifera, L.) as active samplers of airborne particulate matter. PLoS One, 10(7), e0132491. https://doi.org/10.1371/journal.pone.0132491
24. Nelapa, C.A., Swink, W.G., Muerten, P. & Moan, J.E. (2013). Conservative estimates of hunting distance in Cerceris fumipennis Say (Hymenoptera: Crabronidae). Journal of Entomological Science 48: 299–305. https://doi.org/10.18474/0749-8004-48.4.299
25. Papa, G., Capitani, G., Capri, E., Pellecchia, M., & Negri, I. (2021). Vehicle-derived ultrafine particulate contaminating bees and bee products. Science of the Total Environment 750, 141700. https://doi.org/10.1016/j.scitotenv.2020.141700
26. Papa, G., Pellecchia, M., Capitani, G., & Negri, I. (2025). The use of honey bees (Apis mellifera L.) to monitor airborne particulate matter and assess health effects on pollinators. Environmental Science and Pollution Research, 32(16), 10357–10369. https://doi.org/10.1007/s11356-024-33170-8
27. Pérez-Moreno, S., Marcos-García, M.A. & Rojo, S. (2006). Comparative morphology of early stages of two Mediterranean Sarcophaga Meigen, 1826 (Diptera; Sarcophagidae) and a review of the feeding habits of Palaearctic species. Micron 37: 169–179. https://doi.org/10.1016/j.micron.2005.07013
28. Ranjbar, Z., Pourhadadi, D., Montazeri, S., Modaveri, M.R. (2023). Lead compounds in paint and coatings: A review of regulations and latest updates. Progress in Organic Coatings 174, 107247. https://doi.org/10.1016/j.porgcoat.2022.107247
29. Santos, CG., Hartfelder K. (2015). Insights into de dynamics of hind leg development in honey bee (*Apis mellifera* L.) queen and worker larvae- A morpholgy/differential gene expression analysis. Genetics and Molecular Biology 38(3), 263–277. https://dx.doi.org/10.1590/S1415-475738320140393
30. Schraufnagel, D.E. (2020). The health effects of ultrafine particles. Experimental & Molecular Medicine 52, 311–317. https://doi.org/10.1038/s12276-020-0403-3
31. Shewell, G.E. (1987). Sarcophagidae. pp. 1159–1186 in McAlpine, J.F. (Ed.), Manual of Nearctic Diptera, volume 2. Research Branch, Agriculture and Agri-Food Canada, Canada.
32. Shimizu, A. (1997). Taxonomic studies on the Pompilidae ocurring in Japan north of the Ryukyus: the genus Agenioideus Ashmed (Hymenoptera). Japan Journal of Entomology 65: 143–167.
33. Scholz, I., Baumgartner, W., & Federle, W. (2008). Micromechanics of smooth adhesive organs in stick insects: Pads are mechanically anisotropic and softer towards the adhesive surface. Journal of Comparative Physiology A: Neuroethology, Sensory, Neural, and Behavioral Physiology, 194(4), 373–384. https://doi.org/10.1007/s00359-008-0314-6

34. Skaldina, O., Lukowski, A., Leskinen, J.T.T., Koistinen, A.P., Eeva, T. (2023). Mobile samplers of particulate matter-Flying omnivorous insects in detection of industrial contamination. Science of the Total Environment 867, 162511. https://dx.doi.org/10.1016/j.scitotenv.2023.161511
35. Triplehorn, C.A. and Johnson, N.F. (2004) Borror and DeLong's Introduction to the Study of Insects. 7th Edition, Brooks Cole, Pacific Grove.
36. Vincent, J.F.V. and Wegst, U.G.K. (2004). Design and mechanical properties of insect cuticle. Arthropod Structure and Development 33 (3), 187–199.
37. Wagner, T., Neinhuis, C., and Barthlott, W. (1996). Wettability and contaminability of insect wings as a function of their surface sculptures. Acta Zoologica, 77(3), 213–225.
38. Wasbauer, M.S. & Kimsey, L.S. (1985) California Spider Wasps of the Subfamily Pompilinae (Hymenoptera: Pompilidae). Bulletin of the California Insect Survey. Univeristy of California Press, United States.
39. Watson, G.S., Cribb, B.W., Watson, J.A. (2012). Particle Adhesion Measurements on Insect Wing Membranes Using Atomic Force Microscopy. International Scholarly Research Network, ISRN Biophysics. Article ID 947872. https://doi.org/10.5402/2012/947872
40. World Health Organization (2021). WHO Global Air Quality Guidelines: Particulate Matter (PM2.5 and PM10), Ozone, Nitrogen Dioxide, Sulfur Dioxide and Carbon Monoxide. World Health Organization, p. 273. https://apps.who.int/iris/handle/10665/345329
41. Yadav, S., Kumar, Y., Mishra, G., & Lal Jat, B. (2017). Honeybee: Diversity, Castes and Life Cycle. pp. 5–34 in Omkar (Ed.), Industrial Entomology. Springer Nature Singapore.
42. Ye, J., Li, J., Wang, P., Ning, Y., Liu, J., Yu, Q., Bi, X. (2022). Inputs and sources of Pb and other metals in urban area in the post leaded gasoline era. Environmental Pollution 306, 119389. https://doi.org/10.1016/j.envpol.2022.119389

Figures

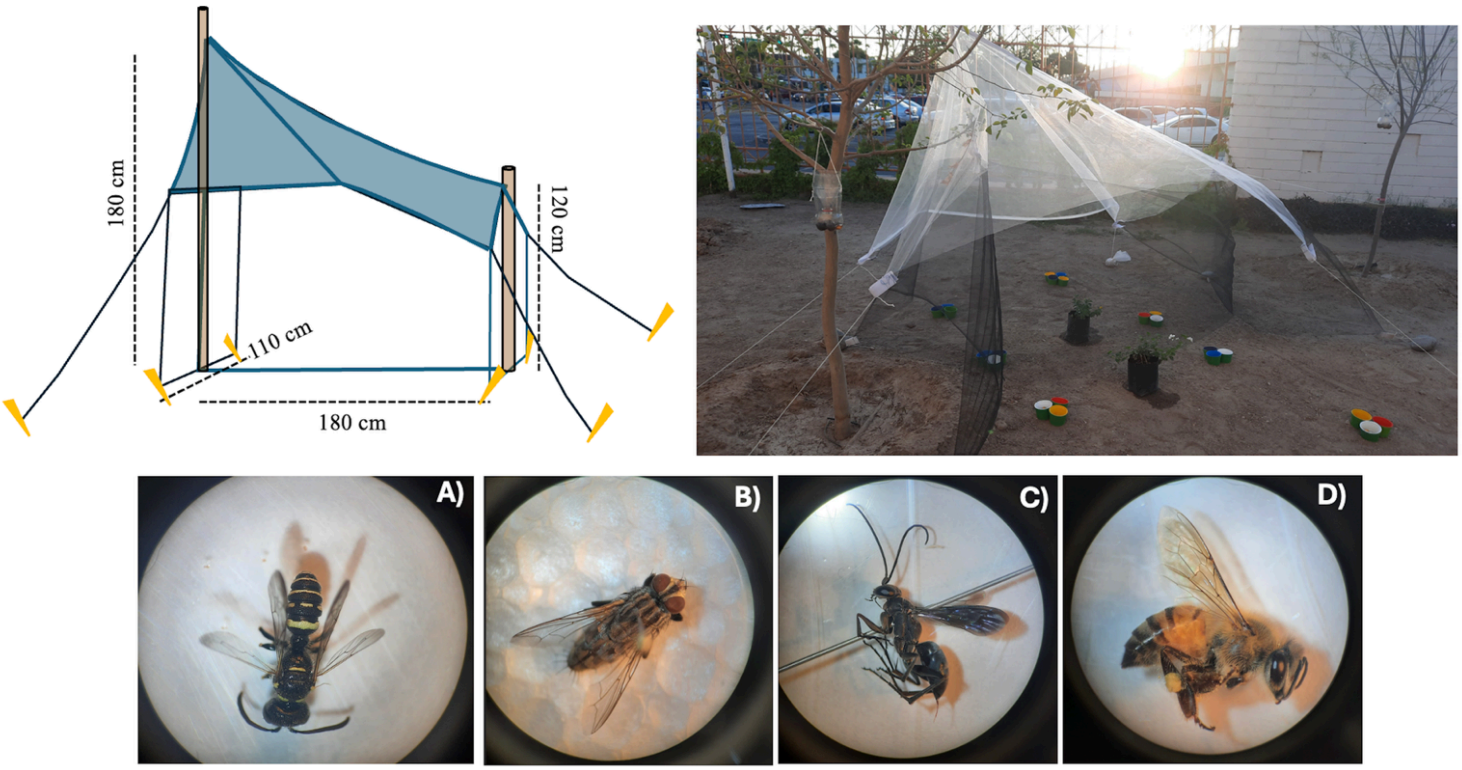


Figure 1

Malaise trap design and photograph of studied site. Collected specimens are (A) wasp *Cerceris sp* (Crabronidae), (B) fly *Sarcophaga sp* (Sarcophagidae), (C) wasp *Agenioideus sp* (Pompilidae), and (D) honey bee *Apis* (Apidae).

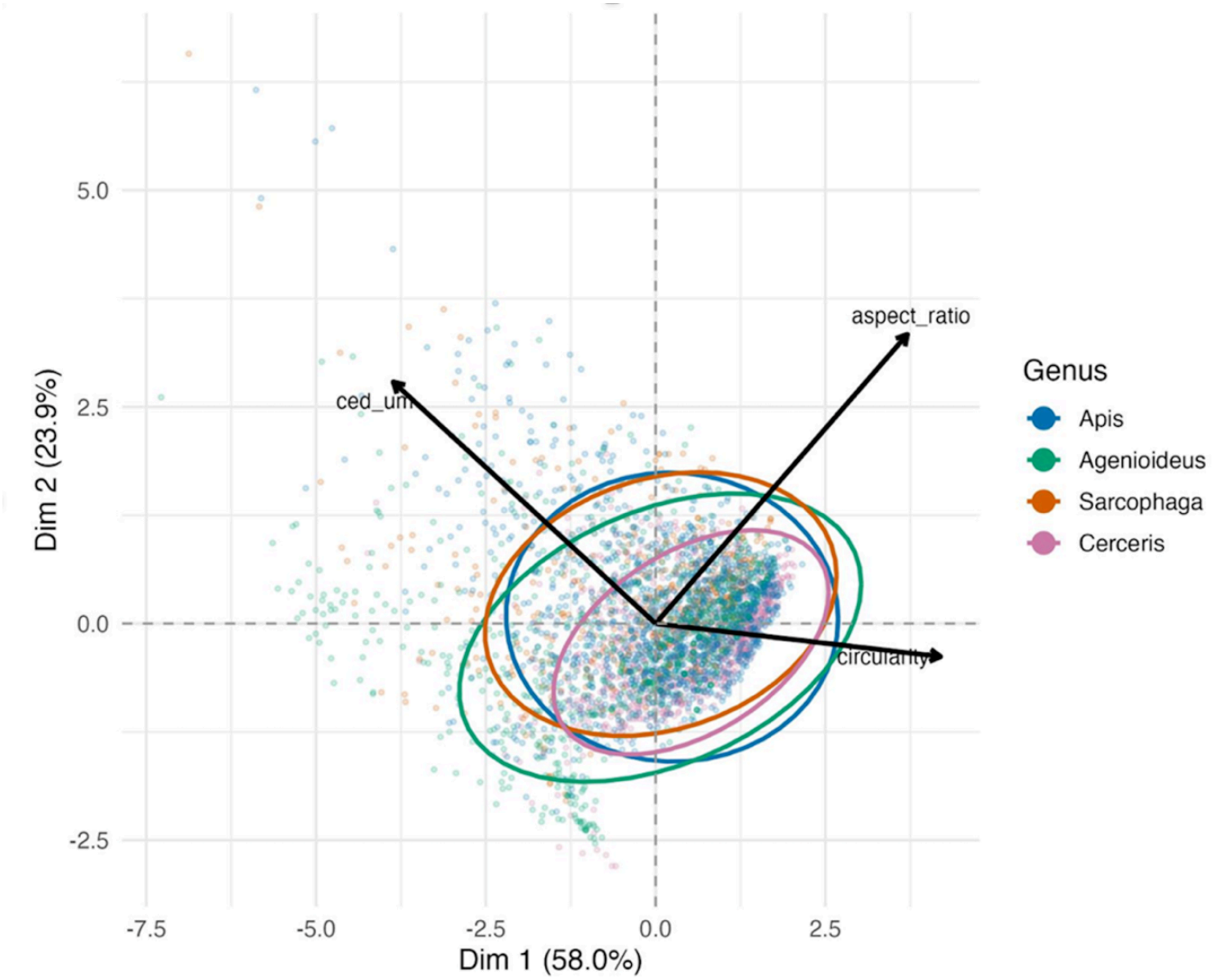


Figure 2

PCA of particle morphometrics.

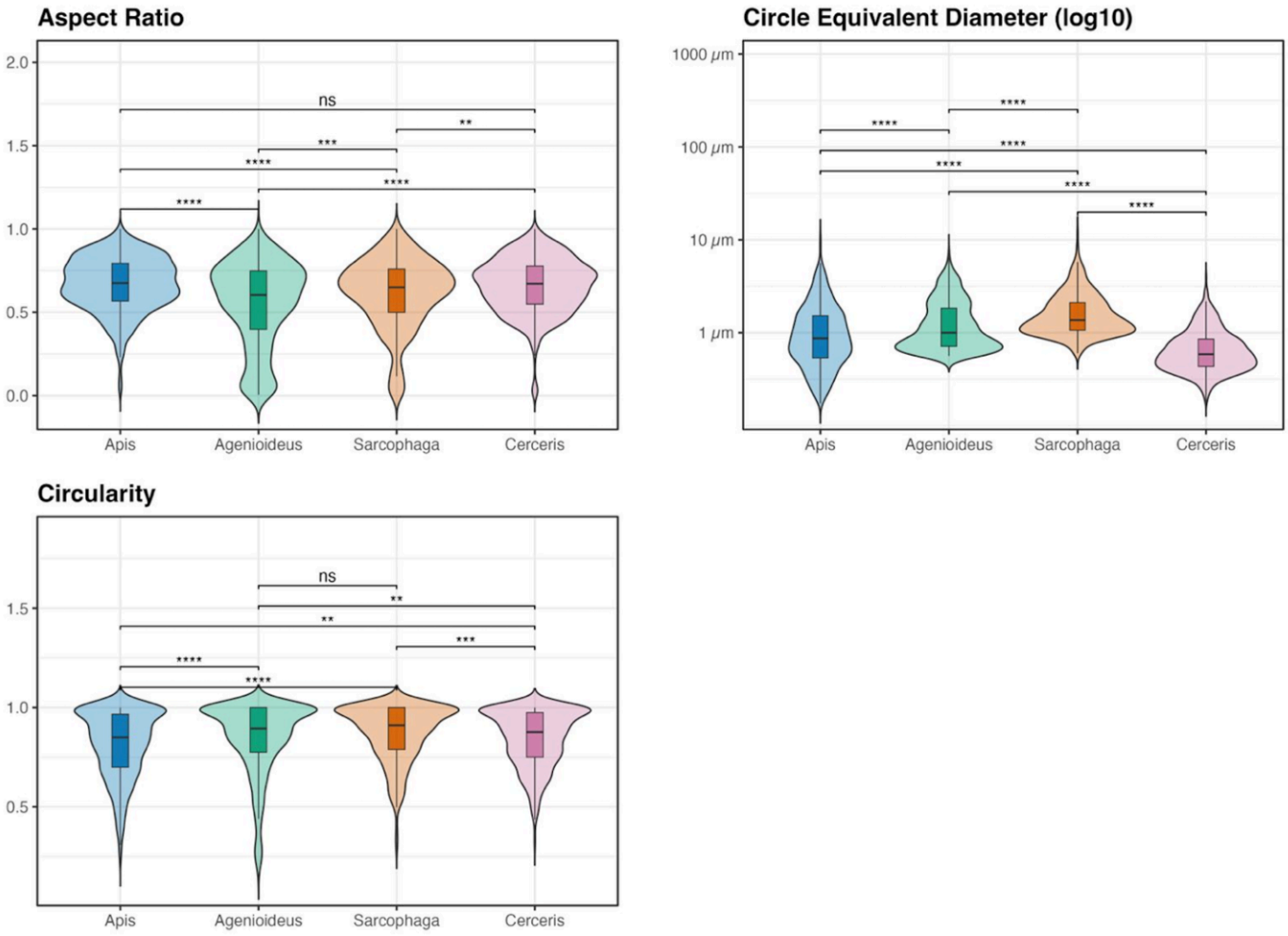


Figure 3

Univariate differences by genus (pairwise posthoc, BH adjusted), µm scale applies only to circle equivalent diameter (log10) panel.

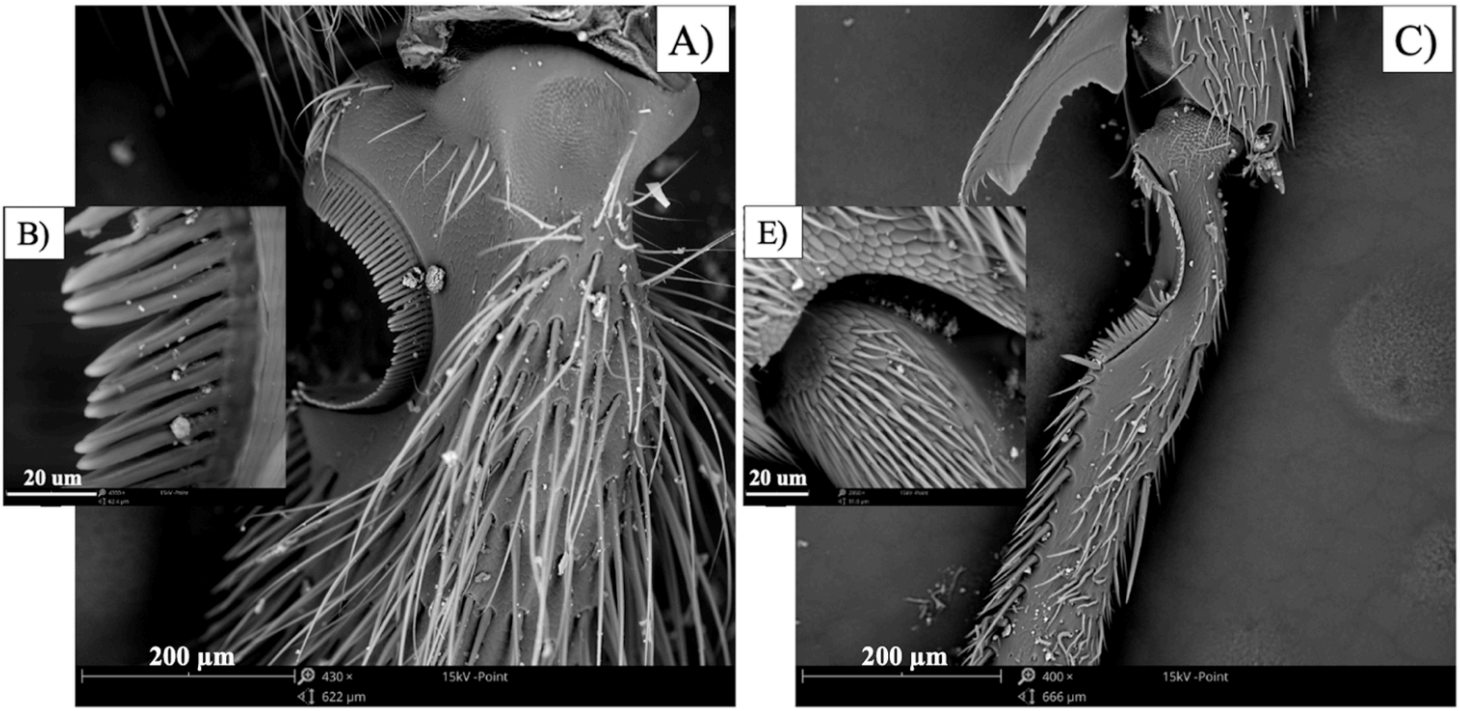


Figure 4

A) SEM image of a leg from *Apis*. B) Augmented image of comb showing submicron particles. C) Image of a leg from *Cerceris*. D) Augmented image of leg from *Cerceris*.

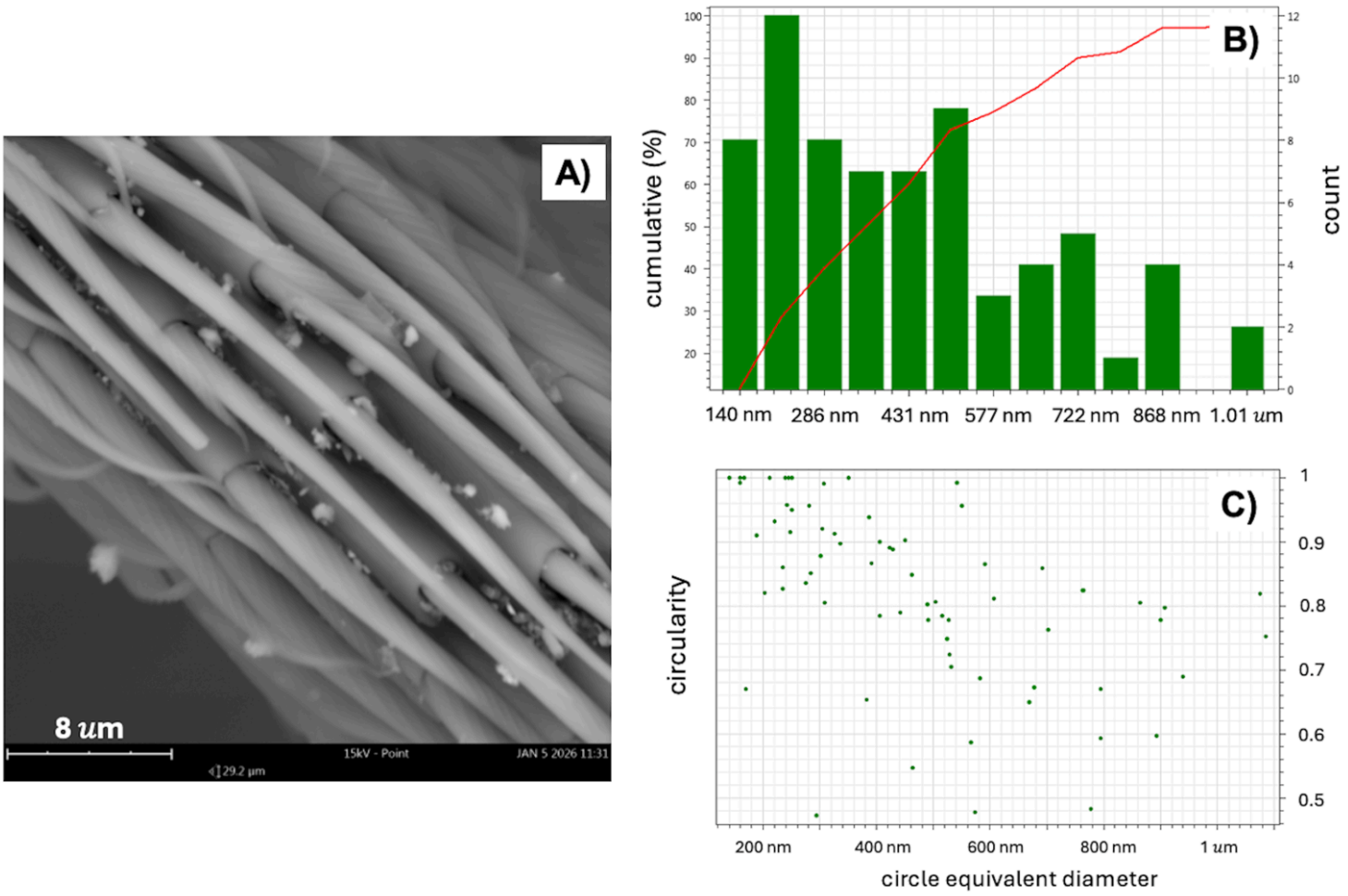


Figure 5

A) Image of a leg from *Cerceris*. B) Histogram of particle size distribution showing submicron range (140 nm to 1 um). C) Size (CED) and circularity of particles detected in legs from *Cerceris*.

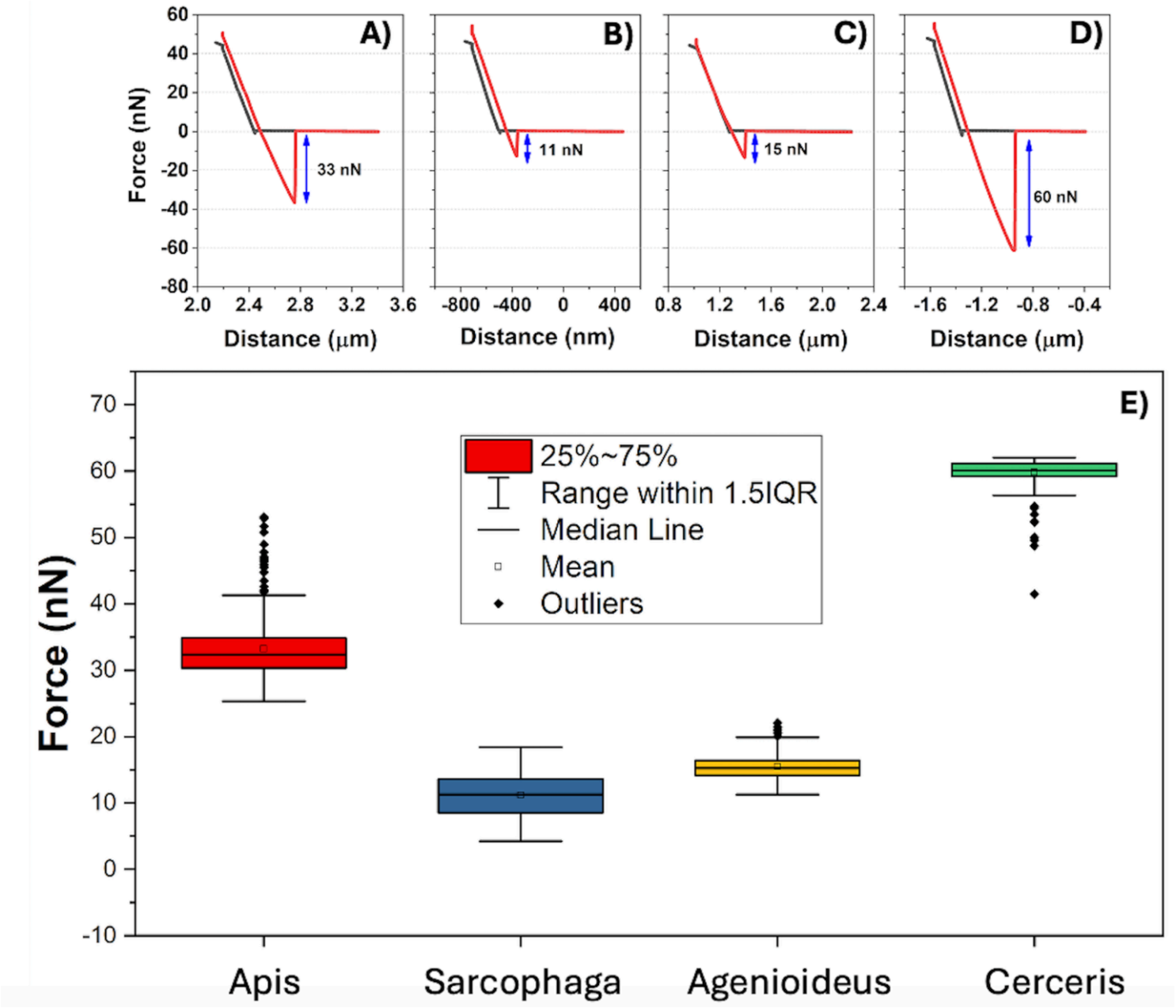


Figure 6

AFM force-distance results for A) *Apis*, B) *Sarcophaga*, C) *Agenioideus*, and D) *Cerceris*. E) Box plots of force (nN) measurements for all studied insects.

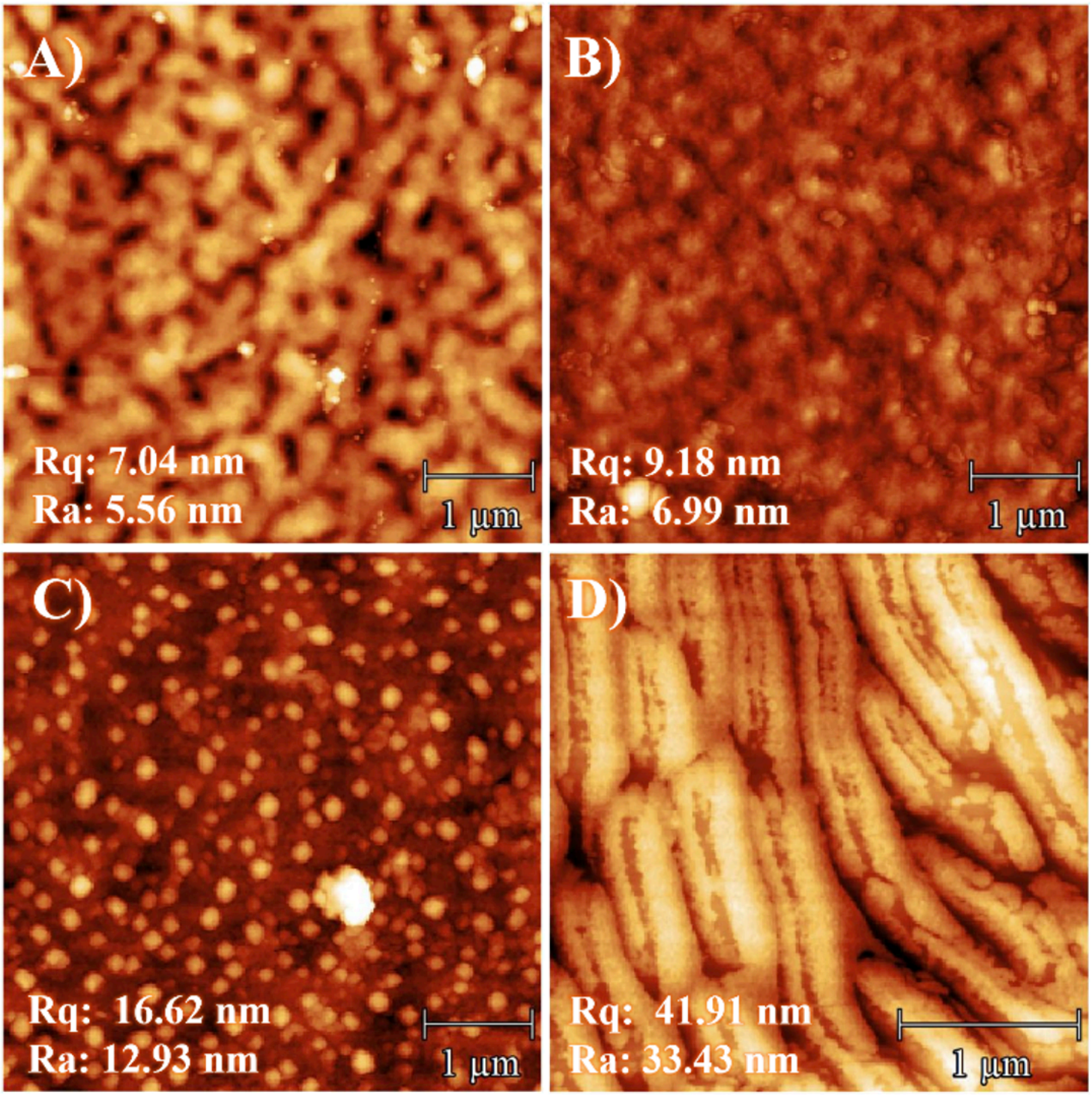


Figure 7

2D AFM topographic images of the wing insect surface for roughness analysis. A) Cerceris, B) Apis, C) Sarcophaga, and D) Agenioideus.

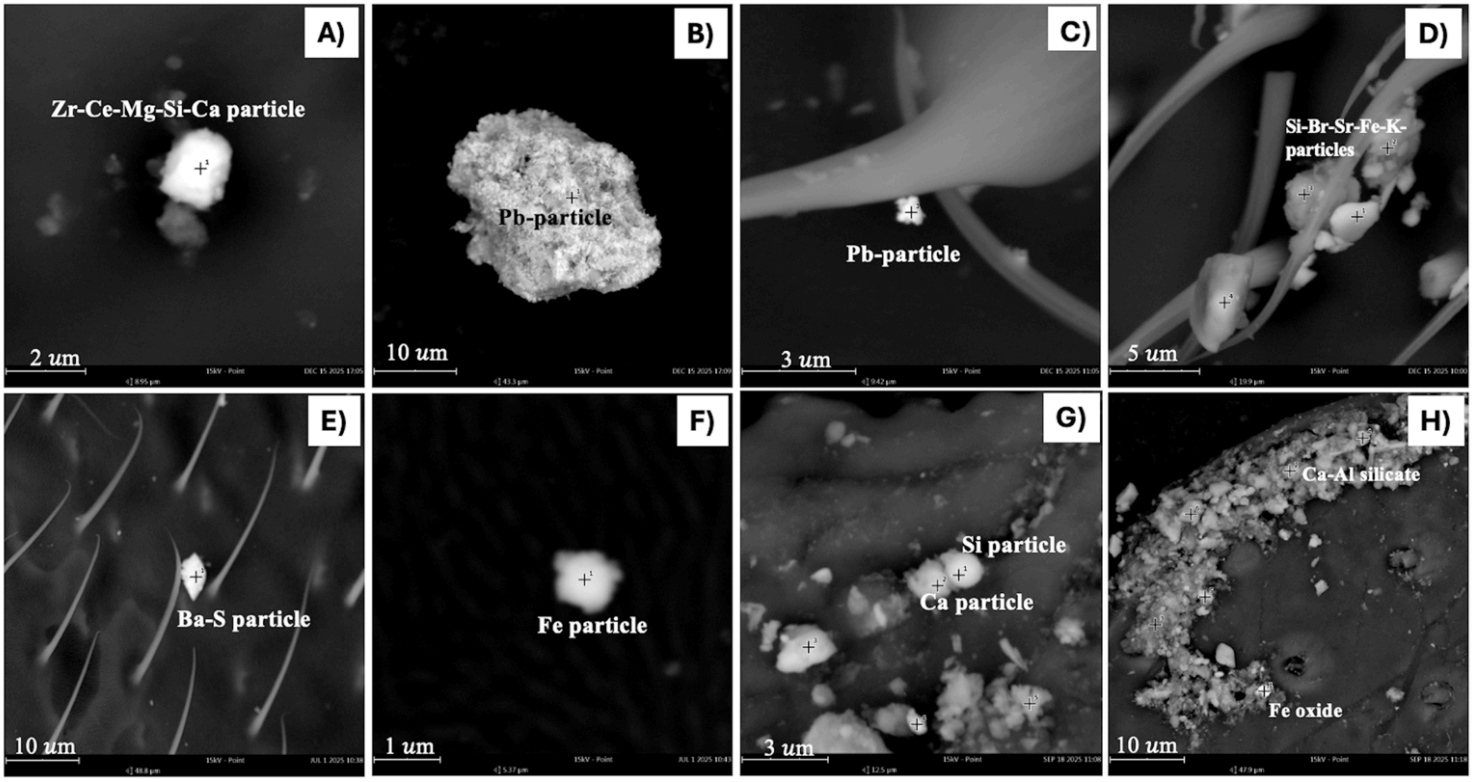


Figure 8

SEM-EDS images of particles in wings from A and B) *Cerceris*, C and D) *Sarcophaga*, E and F) *Agenoioideus*, and G and H) *Apis*.

Supplementary Files

This is a list of supplementary files associated with this preprint. Click to download.

- SupplementaryMaterial.docx